Structural Comparisons of Meizothrombin and Its Precursor Prothrombin in the Presence or Absence of Procoagulant Membranes†

Gang Pei,‡ Thomas M. Laue,§ Ann Aulabaugh,∥ Dana M. Fowlkes,⊥ and Barry R. Lentz*,‡

Department of Biochemistry and Biophysics and Department of Pathology, University of North Carolina, Chapel Hill, North Carolina 27599-7260, Department of Biochemistry, University of New Hampshire, Durham, New Hampshire 03824, and Wellcome Research Laboratories, Research Triangle Park, North Carolina 27709

Received December 19, 1991; Revised Manuscript Received April 1, 1992

ABSTRACT: A stable form of meizothrombin derived from an active-site (Ser^{528}→Ala) mutant of recombinant bovine prothrombin [Pei et al. (1991) *J. Biol. Chem. 266*, 9598–9604] has been used to determine the physical properties and conformation of meizothrombin both in solution and when bound to a procoagulant membrane. As determined with quasi-elastic light scattering, meizothrombin and prothrombin had similar molecular dimensions normal to a membrane (9.4 ± 1.0 nm) and similar binding affinities to procoagulant membranes (1.8 ± 0.2 μM at 0.4 M NaCl). However, meizothrombin had a greater tendency to form oligomers or aggregates in solution. The enhanced oligomerization of meizothrombin was also evidenced by a high apparent z-weighted molecular weight in equilibrium sedimentation experiments at low spin speeds. However, velocity sedimentation experiments performed at high spin speeds demonstrated the same sedimentation coefficient for meizothrombin ($s^0_{20,w}$ = 4.7 ± 0.2 S) as for prothrombin ($s^0_{20,w}$ = 4.7 ± 0.15 S). Circular dichroism measurements revealed minor differences in protein secondary structure between meizothrombin and prothrombin either in the presence or in the absence of phospholipid membranes, as reflected in an increased $\theta_{222}/\theta_{208}$ ratio in meizothrombin relative to prothrombin. The main endotherm of the meizothrombin thermal denaturation profile in a Ca^{2+}-containing buffer, as determined by differential scanning calorimetry, was indistinguishable from that of prothrombin. However, in the presence of phosphatidylserine-containing membranes, the peak temperatures of denaturation profiles of meizothrombin were distinct from those of prothrombin. The detailed changes in the denaturation profile of membrane-bound meizothrombin relative to membrane-bound prothrombin suggested that interdomain interactions may have been less disrupted [Lentz et al. (1991) *Biophys. J. 60*, 942–951] by interaction of meizothrombin with a procoagulant membrane as compared to the behavior of prothrombin. In summary, meizothrombin was found to have an overall configuration, molecular dimension, and secondary structure in solution similar to its precursor prothrombin. However, it mimicked thrombin somewhat in its ease of oligomerization in solution, and it displayed a thermal denaturation profile suggestive of altered interdomain interactions relative to prothrombin when bound to procoagulant membranes.

Meizothrombin is the major intermediate formed during prothrombin activation by prothrombinase (factor X_a and factor V_a assembled in the presence of Ca^{2+} on a phospholipid membrane) in model systems (Rosing et al., 1986; Krishnaswamy et al., 1986, 1987) or on the endothelial cell surface (Tijburg et al., 1991). As an intermediate, meizothrombin bears some properties of its precursor prothrombin and of its derivative thrombin. Having the complete amino acid sequence of prothrombin except for cleavage at a single peptide bond (Arg^{323}–Ile^{324}), meizothrombin is capable of binding to procoagulant phospholipid membranes. Cleavage of Arg^{323}–Ile^{324} in prothrombin, however, leads to partial expression of the active site and confers on meizothrombin full amidolytic activity and partial clotting activity as compared to thrombin (Rosing & Tans, 1988; Doyle & Mann, 1990). Bovine meizothrombin is also able to proteolyze meizothrombin into meizothrombin des fragment 1, and in the case of human meizothrombin, further autolysis occurs to yield thrombin des fragment 3, making meizothrombin quite unstable and difficult to isolate (Rosing & Tans, 1988; Pei & Lentz, 1991).

Instability of meizothrombin as a transient intermediate has been a main obstacle to the study of its physical properties. All previous research on meizothrombin has been conducted in the presence of active-site inhibitors, but even potent irreversible inhibitors could not completely inhibit meizothrombin autolysis (Krishnaswamy et al., 1986, 1987; Armstrong et al., 1990; Doyle & Mann, 1990; Pei & Lentz, 1991). In order to investigate further the molecular interactions of meizothrombin with prothrombinase components, with other coagulation factors, with substrates, and with resting platelets, an active-site mutant (Ser^{528}→Ala) of recombinant bovine prothrombin has been constructed, expressed, and characterized (Pei et al., 1991a). Meizothrombin derived from the mutant prothrombin was stable and did not undergo autolysis, although the mutated active site could still bind a specific thrombin active-site inhibitor *albeit* with a decreased affinity (Pei et al., 1991a).

Previous experiments in this laboratory have demonstrated that prothrombin underwent distinct conformational changes when bound to procoagulant membranes and that the changes

† Supported by USPHS Grants HL45916 (to B.R.L.) and HL36197 and HL31012 (to D.M.F.) and by NSF Grant DIR9002027 (to T.M.L.).

* To whom correspondence should be addressed.

‡ Department of Biochemistry and Biophysics, University of North Carolina.

§ Department of Biochemistry, University of New Hampshire.

∥ Wellcome Research Laboratories.

⊥ Department of Pathology, University of North Carolina.

0006-2960/92/0431-6990$03.00/0

seen on binding to phosphatidylserine (PS)[1]-containing membranes were different from those on binding to phosphatidylglycerol (PG)-containing membranes (Wu & Lentz, 1991; Lentz et al., 1991). These structural changes correlated with an enhanced k_{cat} of thrombin formation catalyzed by the prothrombinase assembled on PS-containing relative to PG-containing membranes (Pei et al., 1991b). This correlation suggests that structural changes in prothrombin may contribute to the ability of procoagulant membranes to enhance prothrombinase activity. The issue of whether related structural changes occur in membrane-bound meizothrombin has not been addressed so far.

In the current study, mutant meizothrombin has been used to determine the physical properties and conformation of meizothrombin both in solution and when bound to a procoagulant membrane. In solution, meizothrombin displayed no significant differences from its precursor prothrombin in sedimentation coefficient and secondary structure, but it mimicked its derivative, thrombin, somewhat in its ease of oligomerization. Meizothrombin also showed molecular dimensions on and binding affinity to procoagulant membranes similar to what has been observed for prothrombin. However, interdomain interactions were altered in meizothrombin relative to prothrombin when bound to a procoagulant phospholipid membrane, as indicated by thermal denaturation profiles.

EXPERIMENTAL PROCEDURES

Materials. Bovine brain phosphatidylserine (PS), dioleoylphosphatidylglycerol (PG), and 1-palmitoyl-2-oleoyl-3-*sn*-phosphatidylcholine (PC) were purchased from Avanti Biochemicals (Birmingham, AL). Snake venom from *Echis carinatus* was obtained from Sigma Chemical (St. Louis, MO) and was coupled to agarose beads (Affi-Gel 10, Bio-Rad) following the instructions provided by Bio-Rad. Isolation of bovine prothrombin and preparation of small unilamellar vesicles (SUV) were as described (Tendian & Lentz, 1990). Large unilamellar vesicles (LUV) were prepared by extrusion as described by Hope et al. (1985). Mutant recombinant bovine prothrombin (Ser^{528}→Ala) was isolated and purified as previously described (Pei et al., 1991a).

Activation of Prothrombin to Meizothrombin. Purified mutant prothrombin was dialyzed against 20 mM Tris, 0.1 M NaCl, and 5 mM Ca, pH 7.6, or in 50 mM 3-(*N*-morpholino)propanesulfonic acid (MOPS), 0.1 mM NaCl, and 5 mM Ca, pH 7.6, buffer, and the agarose bead-linked snake venom was washed thorougly with the corresponding buffer. Typically, 0.7 mg/mL mutant prothrombin was added to the immobilized snake venom (100 μL of dry volume/mL) and was incubated at room temperature. Samples of the activation mixture were withdrawn at time intervals and subjected to analysis by polyacrylamide gel electrophoresis in the presence of sodium dodecyl sulfate (SDS–PAGE) to determine when activation was complete (Pei & Lentz, 1991). When the activation was completed (4–6 h), the agarose bead-linked snake venom was spun down, and the supernatant was stored at −70 °C for the following studies.

Quasi-Elastic Light Scattering. QELS measurements were carried out at an angle of 90° and at room temperature (22 °C) on a light-scattering apparatus constructed by this laboratory around a Nicomp Model 170 computing autocorrelator (Particle Sizing Systems Inc., Santa Barbara, CA), as described in detail by Lentz et al. (1992). LUV composed of PS/PC (20/80) mixtures were titrated with native prothrombin, mutant prothrombin, and mutant meizothrombin in 20 mM Tris, 0.1 M NaCl, and 2 mM $CaCl_2$, pH 7.5, or in 20 mM Tris *0.4 M NaCl*, and 2 mM $CaCl_2$, pH 7.5. All solutions were filtered through 0.2-μm filters (Alltech Associates, Deerfield, IL) before being added to the light-scattering cuvette. The average hydrodynamic radius of a LUV sample or of samples containing LUV–protein complex was obtained as described (Lim et al., 1977; Lentz et al., 1992), with each point defined by at least seven measurements. When EDTA was added to the samples containing protein–LUV complexes, the hydrodynamic radius returned to within 4% of the original LUV value.

From QELS titration data, one can estimate the apparent dissociation constants of protein–LUV complexes by assuming:

$$\text{mass concn of bound protein} = (3/4)\pi(R^3 - R_0^3)\rho N_{LUV} \quad (1)$$

where R_0 is the hydrodynamic radius of LUV alone and R is that of protein–LUV complexes at a certain protein concentration, ρ is the protein specific density (1.37 g/mL; Bajaj et al., 1975), and N_{LUV} is the number concentration of LUV in the sample (obtained from the measured phospholipid concentration and LUV diameter by assuming a bilayer thickness of 50 Å and a membrane density of 0.9 g/cm^3). The free protein concentration can be calculated as $[\text{protein}]_{free} = [\text{protein}]_{total} - [\text{protein}]_{bound}$. The apparent dissociation constants of protein–LUV complexes can be obtained from $[\text{protein}]_{free}$ and $[\text{protein}]_{bound}$ by standard double-reciprocal or Hildebrand analysis.

Sedimentation Equilibrium and Sedimentation Velocity. Sedimentation equilibrium experiments were carried out with the Beckman Model E ultracentrifuge at a constant temperature of 23.3 °C and at speeds of 10 000, 16 000, 24 000, and 32 000 rpm as described by Luckow et al. (1989). Mutant prothrombin and meizothrombin were examined in 50 mM Tris, 0.1 M NaCl, and 2 mM $CaCl_2$, pH 7.6, at four concentrations from 0.15 to 1.2 mg/mL. Both proteins were also examined at 0.6 mg/mL in 50 mM Tris, 0.4 M NaCl, and 2 mM $CaCl_2$, pH 7.6, or in 50 mM Tris, 0.1 M NaCl, and 50 μM Na_2EDTA, pH 7.6. Protein distributions were recorded with Rayleigh interference optics using a 10-mW, 670-nm laser light source. Data were collected directly into a PC computer and analyzed using NONLIN to get the z-average molecular weights, M_z (Johnson et al., 1981; Luckow et al., 1989; Olsen et al., 1991), assuming a partial molar volume for prothrombin of 0.73 mL/g (Bajaj et al., 1975).

Velocity sedimentation experiments were conducted with the Beckman XLA analytical ultracentrifuge at a constant temperature of 20 °C and at a speed of 60 000 rpm (Olsen et al., 1992). Mutant prothrombin and meizothrombin were examined at three concentrations (0.15, 0.3, and 0.6 mg/mL) in 50 mM Tris, 0.1 M NaCl, and 2 mM Ca^{2+}, pH 7.6. Data were collected using absorbance optics (λ = 280 nm), and standardized sedimentation coefficients ($s^0_{20,w}$) were determined as described previously (Williams et al., 1958; Laue & Rhodes, 1990). Transformation of the concentration distribution data to the derivative of the sedimentation coefficient distribution function [$g(s)$] was performed as described by Stafford (1992). In this method, two concentration distribution patterns are subtracted, one from the other, and the radial axis is transformed to the apparent sedimentation

[1] Abbreviations: PS, bovine brain phosphatidylserine; PG, dioleoylphosphatidylglycerol; PC, 1-palmitoyl-2-oleoyl-3-*sn*-phosphatidylcholine; SUV, small unilamellar vesicle(s); LUV, large unilamellar vesicle(s); SDS–PAGE, polyacrylamide gel electrophoresis in the presence of sodium dodecyl sulfate; QELS, quasi-elastic light scattering; M_z, z-average molecular weight; DSC, differential scanning calorimetry; MOPS, 3-(*N*-morpholino)propanesulfonic acid; T_m, midpoint of the thermal transition in degrees Celsius; CD, circular dichroism.

coefficient axis using the relationship:

$$s \simeq \frac{\ln (r/r_m)}{\omega^2 t} \quad (2)$$

where r_m is the radial position of the meniscus, ω is the rotor's angular velocity, and t is the running time from the start of the experiment.

Circular Dichroism Measurements. Circular dichroism (CD) spectra were recorded from 250 to 190 nm on a Jasco J-600 spectropolarimeter (Japan Spectroscopic Co., Tokyo) in a 0.1-cm path-length cell at room temperature (23 °C) with a resolution of 0.2 nm. To minimize scattering effects, the cell was placed adjacent to the photomultiplier window (Schneider & Rosenheck, 1982). Each spectrum is the average of eight scans. The digital data were processed, base-line-corrected, and converted to molar ellipticity, $[\theta]$. Typical protein samples contained approximately 0.15 mg/mL protein (a low concentration was necessary to avoid aggregation artifacts) in 20 mM Tris, 100 mM NaCl, and 5 mM $CaCl_2$, pH 7.5, with or without 0.5 mM PS/PC (20/80) SUV (>90% of prothrombin should be bound at these PS/PC and protein concentrations). Protein concentrations were determined by quantitative amino acid analysis.

Differential Scanning Calorimetry. Differential scanning calorimetry (DSC) measurements were performed on an MC-2 biological microcalorimeter (Microcal, Northampton, MA). The instrumental setup and the sample preparation were as previously described in detailed by Lentz et al. (1991). The protein samples (typically 0.3 mg/mL) for calorimetry scans were in 50 mM MOPS, 100 mM NaCl, and 5 mM $CaCl_2$, pH 7.6. The protein samples were also measured in the presence of 1 mM PS/PC (20/80) LUV. Again, concentrations were chosen to ensure binding of >90% of the protein to membrane surface. The scan rate for all experiments was 45 °C/h. Calorimetric data were converted to heat capacity (kilocalories per mole per degrees kelvin) versus temperature profiles, and endothermic heat capacity peaks were integrated using the continuous base-line algorithm (Sturtevant, 1987). Multiple peaks were deconvolved using software provided by Microcal. These deconvolution algorithms resolve overlapping peaks according to three basic models: (1) independent, two-state transitions; (2) independent, non-two-state transitions; and (3) linked, or sequential, two-state transitions. The least restrictive model (independent, non-two-state transitions) was generally used. In this case, the ratio (R) of the integrated calorimetric enthalpy (ΔH_{cal}, obtained as the integral of a resolved peak) to the van't Hoff enthalpy (ΔH_{vH}, obtained from the magnitude of the peak heat capacity for a resolved peak) for any resolved peak provides information about the nature of the denaturation process associated with that peak (Strurtevant, 1987). A ratio close to 1 indicates a simple, two-state, all-or-nothing denaturation event characteristic of a simple globular protein (Sturtevant, 1987). A ratio greater than 1 indicates that more than one two-state transition is associated with the resolved endotherm. A ratio less than 1 indicates cooperative melting. All samples were measured at least in duplicate and in some cases up to 5 times. Meizothrombin denaturation was monitored at different protein concentrations (as low as 0.09 mg/mL) to check for the potential effects of protein oligomerization on the DSC profile.

RESULTS

Light-Scattering Characterization of the Meizothrombin–Membrane Complex. When PS/PC (20/80) LUV were titrated with mutant prothrombin in 20 mM Tris, 0.1 M NaCl, and 2 mM $CaCl_2$, pH 7.5, the hydrodynamic radius of the protein–membrane complex was found to increase by 9.4 ± 1.0 nm relative to the radius of the PS/PC LUV alone (Figure 1A). This gives a vertical dimension for membrane-bound mutant prothrombin in agreement with the vertical dimension for native prothrombin reported by Schwalbe et al. (1990) (9.0 ± 1.0 nm). When similar vesicles were titrated with mutant meizothrombin under the same conditions, the hydrodynamic radius of meizothrombin–LUV complexes was similar to that of the prothrombin–LUV complexes described above as long as the total protein/phospholipid weight ratio remained less than or equal to 1 (Figure 1A). As more meizothrombin was added, the apparent hydrodynamic radius became unreasonably large, and then the solution slowly turned cloudy, indicative of possible oligomerization or aggregation.

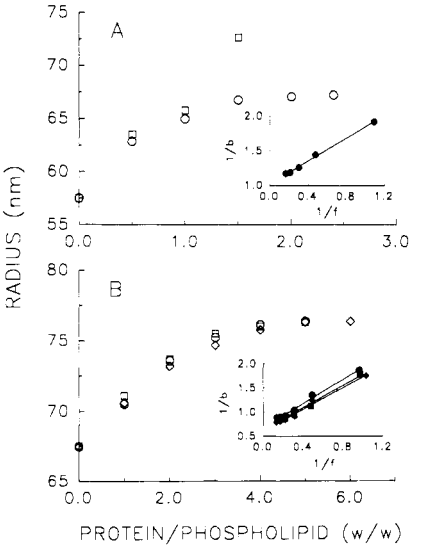

FIGURE 1: Hydrodynamic radius of protein–LUV complexes obtained from QELS measurements. PS/PC (20/80) LUV (0.2 mg/mL) were titrated at room temperature (22 °C) with mutant prothrombin (circles), or mutant meizothrombin (squares), or native bovine prothrombin (diamonds) in 20 mM Tris, 0.1 M NaCl, and 2 mM $CaCl_2$, pH 7.5 (A), or in 20 mM Tris, 0.4 M NaCl, and 2 mM $CaCl_2$, pH 7.5 (B). The inserts in (A) and (B) are the corresponding double-reciprocal plots as described under Experimental Procedures, from which the dissociation constant of the protein–membrane complex is estimated. "*f*" and "*b*" are the protein concentration (micromolar) free in solution and bound to membranes, respectively.

Because of the observed aggregation, we reasoned that meizothrombin might behave in part like thrombin, which is known to agrregate and adhere to surfaces. Thrombin is often isolated and stored at high ionic strength in order to minimize aggregation and surface adsorption. Thus, we increased the ionic strength of the buffer to 0.4 M from 0.1 M NaCl in order to measure the hydrodynamic radius of meizothrombin–LUV complexes. The titration curve thus obtained for mutant meizothrombin was indistinguishable from those obtained for native prothrombin or mutant prothrombin at the same ionic strength (Figure 1B). The results, therefore, indicated that there were no detectable differences between the dimensions and binding of meizothrombin versus prothrombin on procoagulant membranes, at least within the resolution of the QELS method.

The apparent dissociation constants of protein–LUV complexes were estimated from QELS data by means of a standard double-reciprocal plot as described under Experimental Procedures. A value of 0.8 ± 0.2 μM for mutant prothrombin was obtained (insert in Figure 1A), similar to that reported under comparable ionic conditions for native prothrombin (0.5 μM; Nelsestuen & Broderius, 1977). The constants obtained at higher ionic strength (insert in Figure 1B) for

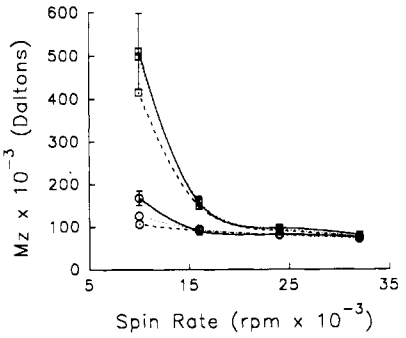

FIGURE 2: Apparent z-average gram molecular weights (M_z), as acquired from sedimentation equilibrium experiments, of mutant prothrombin and meizothrombin as a function of the spin rate. At a constant temperature of 23.3 °C, mutant prothrombin (circles) and meizothrombin (squares) were examined in 50 mM Tris, 0.1 M NaCl, and 2 mM $CaCl_2$, pH 7.6 (solid lines), at four concentrations from 0.15 to 1.2 mg/mL, from which the means and standard deviations were calculated. Both proteins were also examined at 0.6 mg/mL in 50 mM Tris, 0.4 M NaCl, and 2 mM $CaCl_2$, pH 7.6 (dashed lines), or in 50 mM Tris, 0.1 M NaCl, and 50 μM EDTA, pH 7.6 (dotted lines).

native prothrombin, mutant prothrombin, or meizothrombin were 1.7 ± 0.2, 1.9 ± 0.2, and 1.8 ± 0.2 μM, respectively. These values compare with a value of approximately 1.8 μM estimated from the report of Resnick and Nelsestuen (1980) for bovine prothrombin under similar ionic conditions. It appears that the binding of mutant meizothrombin to PS/PC LUV is indistinguishable from the binding of mutant or native prothrombin to the same vesicles.

Oligomerization of Meizothrombin. Equilibrium sedimentation of mutant prothrombin (circles in Figure 2) suggested that it underwent oligomerization, as evidenced by the decreased apparent molecular weight with increased rotor speed (Roark & Yphantis, 1969; Yphantis et al., 1978). This behavior is typical of native prothrombin (Luckow et al., 1989; Lyons et al., 1990; Laue, unpublished observation). As with native prothrombin (Luckow et al., 1989; Lyons et al., 1990), the extent of oligomer formation was [Ca^{2+}]-dependent for mutant prothrombin (Figure 2). In the presence of 2 mM $CaCl_2$, oligomer formation was reduced substantially by increasing the ionic strength to 0.4 M NaCl (Figure 2).

Equilibrium sedimentation of meizothrombin also revealed heterogeneity (squares in Figure 2), but with differences as compared to mutant prothrombin. First, the meizothrombin formed much larger oligomers than did prothrombin (Figure 2). Moreover, oligomer formation was not [Ca^{2+}]-dependent and was less affected by increasing the ionic strength to 0.4 M NaCl (Figure 2). The steep decrease in the z-average molecular weight (M_z) with increasing rotor speed suggested the presence of a small amount of large oligomers or even aggregates.

Sedimentation Coefficient of Mutant Prothrombin and Meizothrombin. In the presence of 2 mM $CaCl_2$, mutant prothrombin sedimented as a single boundary at $s^0_{20,w}$ = 4.7 ± 0.15 S. More detailed analysis of the boundary shape revealed a single boundary broadening well in excess of that expected for diffusion (Hayes & Laue, 1990; Hayes, 1991) but no separate, second boundary. This behavior is identical to that of native prothrombin (Jackson et al., 1979). Meizothrombin also exhibited a single, although somewhat broader, boundary, with $s^0_{20,w}$ = 4.7 ± 0.2 S. Detailed analysis of the boundary shape revealed more severe heterogeneity than was observed for prothrombin. This is evident in Figure 3, wherein is shown the first derivative of the sedimentation coefficient distribution function [$g(s)$] as a function of the sedimentation coefficient. Mutant prothrombin (points) and mutant meizothrombin (solid line) showed identical behavior for the main population of particles in these samples ($s^0_{20,w}$ = 4.7 S). However, the mutant meizothrombin sample showed a small but significant population of particles with a broad range of sedimentation coefficients centered about 18 S. This indicates that the mutant meizothrombin sample contained a minor population of particles with gram molecular weight in excess of 500 000 daltons, in complete agreement with the equilibrium sedimentation measurements repeated above.

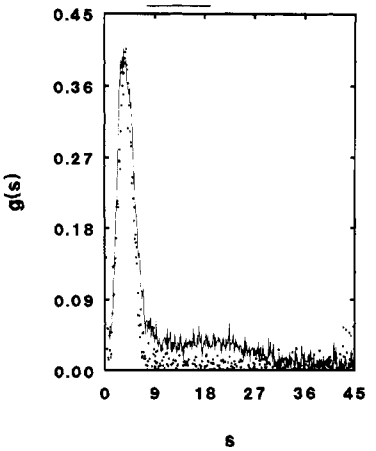

FIGURE 3: First-derivative sedimentation coefficient distributions for mutant prothrombin (points) and meizothrombin (solid line) made by subtracting consecutive, unsmoothed absorbance scans collected 300 s apart and normalized to the plateau absorbance ($A_{280} \approx 0.45$ for each protein). Data were acquired at 20 °C and 60 000 rpm. The reduced sedimentation time ($\omega^2 t$) needed for the computation of s was taken as the midpoint between the two scans and corresponds to 4.457 × 10^{10} s^{-1} for prothrombin and 3.654 × 10^{10} s^{-1} for meizothrombin. Presented here are sedimentation coefficients which have not been corrected for solution viscosity and density to standard conditions (H_2O at 20 °C). The positions of the major peaks (mutant prothrombin = 4.45 S and meizothrombin = 4.47 S), when corrected, are at 4.7 S, which is identical to that for native prothrombin.

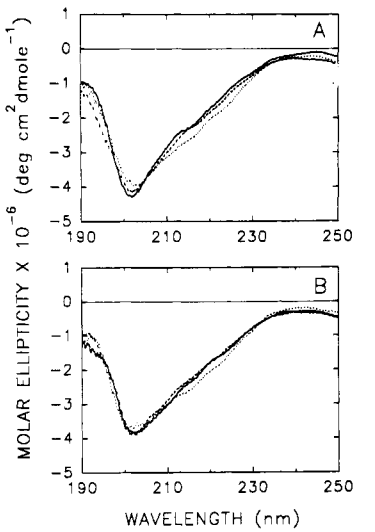

FIGURE 4: CD spectra of native prothrombin (solid line), mutant prothrombin (dashed line), and mutant meizothrombin (dotted line). The protein samples of 0.15 mg/mL were measured at room temperature (23 °C) in 20 mM Tris, 100 mM NaCl, and 5 mM $CaCl_2$, pH 7.5 (A), or in the same buffer but in the presence of 0.5 mM PS/PC (20/80) SUV (B).

Secondary Structure from CD Spectra. The CD spectrum of meizothrombin displayed the same overall shape as that of native prothrombin or mutant prothrombin either in the absence (Figure 4A) or in the presence (Figure 4B) of PS/PC SUV. The molar ellipticity of meizothrombin was, in both cases, less negative at the minimum, 202–206 nm, and more negative around 210–230 nm than the corresponding values

Table I: $\theta_{222}/\theta_{208}$ Ratio from CD Measurements for Prothrombins and Meizothrombin in the Absence or Presence of PS/PC (20/80) SUV[a]

sample	$\theta_{222}/\theta_{208}$[b]
protein	
native prothrombin[c]	0.47/0.50
mutant prothrombin[c]	0.49/0.51
mutant meizothrombin[c]	0.55/0.57
protein + PS/PC SUV	
native prothrombin	0.50
mutant prothrombin	0.51
mutant meizothrombin	0.57

[a] Experimental conditions were as described in the legend of Figure 4. [b] Ratio of molar ellipiticity (in degrees centimeter squared per decimole) at 222 nm to that at 208 nm. [c] Data were from duplicate measurements, as shown.

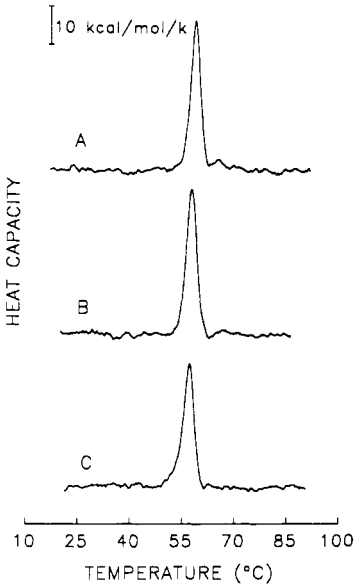

FIGURE 5: Thermal denaturation profiles of native and mutant prothrombin and mutant meizothrombin from DSC. The protein samples (0.3 mg/mL) of bovine prothrombin (A), mutant prothrombin (B), and mutant meizothrombin (C) were examined at a scan rate of 45 °C/h in 50 μM MOPS, 100 mM NaCl, and 5 mM $CaCl_2$, pH 7.6.

for native prothrombin and mutant prothrombin. This was reflected in the value of $\theta_{222}/\theta_{208}$ (Table I), a parameter which is sensitive to the amount of α-helix (a value of approximately 1.1 corresponds to 100% helical content; Greenfield & Fasman, 1969). This ratio was ca. 12% greater for mutant meizothrombin than for mutant prothrombin, a difference that was clearly greater than the error in reproducing these experiments (see Table I). The increase in $\theta_{222}/\theta_{208}$ indicated a somewhat higher helical content in meizothrombin compared to its parent prothrombin.

When either prothrombin or its derivative meizothrombin were bound to PS/PC membranes, no change was detected in the secondary structure of either protein. This disagrees with our earlier Fourier transform infrared analysis of native prothrombin (Wu & Lentz, 1991) that showed a small decrease (5%) in random-coil conformations accompanied by very small and barely measurable increases in α-helix (2%) and β-sheet (3%) content upon binding to PS/PC membranes. Such a small change in α-helix content is apparently beyond the detection limit of our CD methods.

DSC Thermal Denaturation Profiles. Representative thermal denaturation profiles are presented in Figure 5 for native prothrombin (A), mutant prothrombin (B), and mutant meizothrombin (C). The overall shapes of all three profiles appeared similar except that the midpoint temperature (T_m) of the main endotherm (peak 1) for mutant prthrombin or meizothrombin was 1 °C lower than that for native prothrombin (Table II). There were no significant differences between mutant prothrombin (B) and meizothrombin (C) in terms of the T_m and the calorimetric enthalpy (ΔH_{cal}) of the main endotherm (peak 1). A second, minor endotherm (peak 2) was barely perceptible above base line at temperatures just above the main endotherm. Although this endotherm could not be adequately characterized from scans made on prothrombin at 0.3 mg/mL concentration, when native or mutant prothrombin was scanned at a higher protein concentration (0.9 mg/mL, data not shown), the high-temperature endotherm (peak 2) was clearly presented, consistent with the profile reported previously (Lentz et al., 1991). Peak 2 characteristics of prothrombin from these higher concentration experiments are summarized in Table II. Although the high-temperature endotherm (peak 2) was less easily resolved in the low concentration scans for prothrombin (frames A and B in Figure 5), it could not be detected at all for meizothrombin, although a slight shoulder was evident on the low-temperature edge of the main endotherm (Figure 5C). Unfortunately, sample aggregation made it impractical to perform scans with meizothrombin at 0.9 mg/mL, making it impossible to confirm that the peak 2 endotherm was missing or shifted to lower temperatures for meizothrombin.

In the presence of PS/PS (20/80) LUV (1 mM) as shown in Figure 6, the T_m of the main endotherm (peak 1) of native prothrombin (A) or mutant prothrombin (B) was shifted about 2 °C lower relative to its position when prothrombin was denatured in the absence of PS/PC LUV (Table II). However, the T_m of the main endotherm of mutant meizothrombin was lowered only about 1 °C relative to meizothrombin in the absence of PS/PC LUV. In other words, the main endotherm associated with meizothrombin denaturation was lowered less dramatically by membrane binding than was the main endotherm for prothrombin. Further comparison between mutant prothrombin and mutant meizothrombin profiles in the presence of PS/PC LUV revealed that the T_m of meizothrombin's minor endotherm (peak 2) was higher and the calorimetric to van't Hoff ratio (R) was lower than that of mutant prothrombin. These differences between the effects of membrane binding on mutant prothrombin and mutant meizothrombin suggest different alterations of interdomain interactions (Lentz et al., 1991) in meizothrombin as compared to prothrombin associated with binding to procoagulant membranes.

Note that meizothrombin, when denatured at a concentration of 0.09 mg/mL in the presence of PS/PC LUV, showed the same T_m for the main endotherm as when examined at 0.3 mg/mL (Table II), arguing against the potential effect of meizothrombin oligomerization or aggregation on the denaturation profile. Also arguing against artifacts induced by irreversible aggregation events during prothrombin denaturation is the minimal dependence of T_m on scan rate that we have reported previously (Lentz et al., 1991).

DISCUSSION

Since meizothrombin was first identified as a major intermediate in prothrombin activation by the full prothrombinase in vitro and presumably also in vivo, very few reports have appeared on its biochemical and biophysical properties. This can be attributed mainly to the instability of meizothrombin toward autolysis; even potent active-site inhibitors did not completely block autolysis (Armstrong et al., 1990; Dolye & Mann, 1990; Pei & Lentz, 1991). In the study reported here, a stable form of meizothrombin derived from

Table II: Thermotropic Characteristics of Prothrombins and Meizothrombin in the Absence or Presence of PS/PC (20/80) LUV by Deconvolution Analysis[a]

sample	peak 1			peak 2		
	T_m[b]	ΔH_{cal}[c]	R[d]	T_m	ΔH_{cal}	R
protein						
native prothrombin	58.2	182	0.8	65.4[f] (65)	103[f]	2.0[f]
mutant prothrombin	57.3	188	0.9	66.4[f] (66)	91[f]	2.1[f]
mutant meizothrombin	56.9	185	0.9	*h*	*h*	*h*
protein + PS/PC LUV[e]						
native prothrombin	56.2	141	0.6	71.4	100	2.3
mutant prothrombin	55.1	176	1.1	70.6	60	1.3
mutant meizothrombin	56.1	187	1.0	74.3	48	0.6
mutant meizothrombin	56.2[g]					

[a] Unless indicated, measurements were performed at 0.3 mg/mL protein and at scan rate of 45 °C/h, and in the presence of 5 mM $CaCl_2$. [b] T_m is the midpoint of the transition in degrees Celsius, with an uncertainty of ±0.2 °C. [c] ΔH_{cal} is the calorimetric enthalpy in kilocalories per mole, with an uncertainty of ±15 kcal/mol. [d] R is the ratio of the calorimetric to van't Hoff enthalpy, $\Delta H_{cal}/\Delta H_{vH}$. [e] Fit was improved by relaxing the two-state assumption for protein plus PS/PC LUV. [f] Measured at a protein concentration of 0.9 mg/mL. [g] Measured at a protein concentration of 0.09 mg/ml. [h] A peak was not resolved.

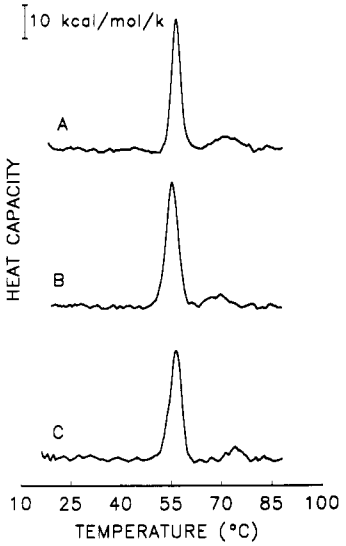

FIGURE 6: Thermal denaturation profiles of native and mutant prothrombin and meizothrombin in the presence of PS/PC (20/80) LUV. The protein samples (0.3 mg/mL) of bovine prothrombin (A), mutant prothrombin (B), and mutant meizothrombin (C) were measured, in the presence of 1 mM PS/PC LUV, at a scan rate of 45 °C/h in 50 μM MOPS, 100 mM NaCl, and 5 mM $CaCl_2$, pH 7.6.

an active-site mutant (Ser^{528}→Ala) of recombinant bovine prothrombin has been used to obtain structural information on meizothrombin both free in solution and when bound to PS/PC procoagulant membranes. The mutant meizothrombin, although devoid of any enzymatic activity, still bound a specific thrombin active-site inhibitor, dansylarginine *N,N*-(3-ethyl-1,5-pentanediyl)amide. This fluorescent inhibitor, when bound to mutant meizothrombin, exhibited a fluorescence spectrum similar to that of inhibitor bound to native meizothrombin (Pei et al., 1991a).

The meizothrombin molecule in aqueous solution, with its active site exposed, displayed hydrodynamic properties (sedimentation coefficient and apparent molecular weight) similar to the prothrombin molecule. Observed differences in the apparent molecular weight determined by equilibrium sedimentation at lower spin rates (Figure 2) were apparently a reflection of enhanced meizothrombin oligomer formation as compared to prothrombin. Since the z-average molecular weight is obtained from equilibrium sedimentation experiments using our methods of detection and analysis, a small amount of oligomer formation would greatly alter the apparent molecular weight. High spin rates apparently tend to clear the aggregates, leading to a reasonable estimate of M_z (see Figure 2). For velocity sedimentation experiments, too, the high spin rate of 60 000 rpm should have cleared the sample of larger aggregates quickly, leading to a reasonable estimate of the sedimentation coefficient. However, when the moving boundary shape was analyzed quantitatively, as shown in Figure 3, a clear indication of meizothrombin aggregation was evident even in velocity sedimentation experiments.

Our light-scattering data also gave evidence of meizothrombin aggregation in the presence of PS/PC membranes. The mechanism of meizothrombin aggregation in the presence of the phospholipid surface, however, may be dissimilar from that of oligomerization in aqueous solution. Interactions of meizothrombin with the surface due to exposure of the active site may be involved, as may be meizothrombin-mediated vesicle–vesicle interactions. We have dealt with the problem of aggregation either by increasing the ionic strength, by using pH 7.6 instead of pH 7.4 (Luckow et al., 1989), or by using a low meizothrombin concentration. When measured at 0.4 M NaCl (Figure 1B), meizothrombin presented the same molecular dimension on and the same binding affinity for the phospholipid surface as did prothrombin. This was not surprising, since both prothrombin and meizothrombin possess an intact fragment 1 region, which is largely responsible for binding to procoagulant membranes.

CD measurements have also failed to detect changes in meizothrombin (and, for that matter, prothrombin) secondary structure upon binding to PS/PC membranes. Although our previous Fourier transform infrared studies did manage to detect small secondary structural changes in prothrombin upon binding to PS/PC membranes, the sensitivity of meizothrombin to aggregation has made such experiments impossible on this partially activated form of prothrombin. For the purpose of this study, however, it is still possible to say that meizothrombin showed no detectable differences relative to prothrombin in secondary structure adjustments associated with binding to procoagulant membranes.

The results of differential scanning calorimetry measurements revealed some minor but detectable differences between the response to membrane binding of mutant prothrombin and mutant meizothrombin. These differences are revealed by comparing Figures 5 and 6 and are summarized in Table II. For both proteins, a significant endotherm appeared at high temperature when they were denatured in a membrane-bound state. We have shown previously (Lentz et al., 1991) that, for native bovine prothrombin, this endotherm consisted of two peaks (see R = 2.3 in Table II), one demonstrated to correspond to the melting of membrane-bound fragment 1, the N-terminal third of prothrombin thought to be responsible for membrane binding. The other high-temperature en-

dotherm was hypothesized to reflect the melting of the fragment 2 domain of prothrombin, a 12 000-dalton joiner region between fragment 1 and the domain that ultimately becomes thrombin (termed prethrombin 2; prethrombin 2 attached to fragment 2 is termed prethrombin 1). The present results make it appear that the fragment 2 domain of the mutant molecule is not stabilized to the same extent by membrane binding as in the native molecule (note that the peak 1 enthalpy is not reduced and that the R value for peak 2 is not close to 2). This could reflect either altered folding of the prothrombin expressed in cultured CHO cells or an altered conformation of prothrombin associated with the single Ser^{528}→Ala mutation. Previously, we have shown that expressed wild-type prothrombin was carboxylated the same as native prothrombin and was activated by the membrane-assembled prothrombinase with the same kinetics as was native prothrombin (Pei et al., 1991a). This argues against altered folding during expression. Our earlier work also showed that the mutant prothrombin was activated decidedly more slowly by the full, membrane-assembled prothrombinase than were the wild-type or native proteins, although all three were activated equivalently by two snake venoms that do not require assembly on a membrane surface (Pei et al., 1991a). Our current denaturation results taken together with our published activation studies suggest that mutation of the active-site Ser^{528} alters the conformation of membrane-bound prothrombin in such a way that activation of prothrombin by the prothrombinase is altered.

Despite the above noted differences between mutant and native prothrombin, the T_m of peak 1 was shifted to lower temperature by membrane binding in mutant prothrombin to the same extent as in native prothrombin (2–2.2 °C). Our previous interpretation was that membrane binding disrupted interactions between the fragment 2 domain and the prethrombin 2 and fragment 1 domains (Lentz et al., 1991). In mutant meizothrombin, peak 1 was shifted lower by only 0.8 °C by membrane binding. In the context of our previous studies, this difference in the response to membrane binding of mutant prothrombin and meizothrombin might be interpreted in terms of less severe alterations in interdomain interactions within the membrane-bound meizothrombin molecule than within prothrombin when it binds to membranes. This interpretation is necessarily vague, as it is not possible to derive precise structural information from thermodynamic data. At this point, it is possible only to say that membrane binding induces similar conformational shifts in both prothrombin and meizothrombin but that these changes are less severe in the case of meizothrombin. More defined structural information remains to be pursued by methods having greater resolving power, such as fluorescence resonance energy transfer and X-ray crystallography.

REFERENCES

Armstrong, S. A., Husten, E. J., Esmon, C. T., & Johnson, A. E. (1990) *J. Biol. Chem. 265*, 6210–6218.

Bajaj, S. P., Butkowski, R. J., & Mann, K. G. (1975) *J. Biol. Chem. 250*, 2150–2156.

Doyle, M. F., & Mann, K. G. (1990) *J. Biol. Chem. 265*, 10693–10701.

Greenfield, N., & Fasman, G. D. (1969) *Biochemistry 8*, 4108–4116.

Hayes, D. B., & Laue, T. M. (1990) *Biophys. J. 57*, 573a.

Hays, D. B. (1991) M.S. Thesis, University of New Hampshire, Durham, NH.

Hope, M. J., Bally, M. B., Webb, G., & Cullis, P. R. (1985) *Biochim. Biophys. Acta 812*, 55–65.

Jackson, C. M., Peng, C. W., Brenkle, G. M., Jonas, A., & Stenflo, J. (1979) *J. Biol. Chem. 254*, 5020–5026.

Johnson, M. L., Correia, J. C., Yphantis, D. A., & Halvorson, H. R. (1981) *Biophys. J. 36*, 575–588.

Krishnaswamy, S., Mann, K. G., & Nesheim, M. E. (1986) *J. Biol. Chem. 261*, 8977–8984.

Krishnaswamy, S., Church, W. R., Nesheim, M. E., & Mann, K. G. (1987) *J. Biol. Chem. 262*, 3291–3299.

Laue, T. M., & Rhodes, D. G. (1990) *Methods Enzymol. 182*, 566–587.

Lentz, B. R., Wu, J. R., Sorrentino, A. M., & Carleton, J. M. (1991) *Biophys. J. 60*, 942–951.

Lentz, B. R., McIntyre, G. F., Parks, D. J., Yates, J. C., & Massenburg, D. (1992) *Biochemistry 31*, 2643–2653.

Lim, T. K., Bloomfield, V. A., & Nelsestuen, G. L. (1977) *Biochemistry 16*, 4177–4181.

Luckow, E. A., Lyons, D. A., Ridgeway, T. M., Esmon, C. T., & Laue, T. M. (1989) *Biochemistry 28*, 2348–2354.

Lyons, D. A., Esmon, C. T., Nelsestuen, G. L., & Laue, T. M. (1990) *Biophys. J. 57*, 416a.

Nelsestuen, G. L., & Broaderius, M. (1977) *Biochemistry 16*, 4172–4177.

Olsen, P. H., Esmon, N. L., Esmon, C. T., & Laue, T. M. (1992) *Biochemistry 31*, 746–754.

Pei, G., & Lentz, B. R. (1991) *Blood Coagulation Fibrinolysis 2*, 309–316.

Pei, G., Baker, K., Emfinger, S. M., Fowlkes, D. M., & Lentz, B. R. (1991a) *J. Biol. Chem. 266*, 9598–9604.

Pei, G., Powers, D. D., & Lentz, B. R. (1991b) *Thromb. Haemostasis 65*, 664a.

Resnick, R. M., & Nelsestuen, G. L. (1980) *Biochemistry 19*, 3028–3033.

Roark, D. E., & Yphantis, D. A. (1969) *Ann. N.Y. Acad. Sci. 164*, 245–278.

Rosing, J., & Tans, G. (1988) *Thromb. Hemostasis 60*, 355–360.

Rosing, J., Zwaal, R. F. A., & Tans, G. (1986) *J. Biol. Chem. 261*, 4224–4228.

Schneider, A. S., & Rosenheck, K. (1982) *Tech. Life Sci. B424*, 1–26.

Schwalbe, R., Dahlbäck, B., Hillarp, A., & Nelsestuen, G. (1990) *J. Biol. Chem. 265*, 16074–16081.

Stafford, W. F. (1992) *Anal. Biochem. 203*, 295–301.

Sturtevant, J. M. (1987) *Annu. Rev. Phys. Chem. 38*, 463–488.

Tendian, S. W., & Lentz, B. R. (1990) *Biochemistry 29*, 6720–6729.

Tijburg, P. N. M., van Heerde, W. L., Leenhouts, H. M., Hessing, M., Bouma, B. N., & de Groot, P. G. (1991) *J. Biol. Chem. 266*, 4017–4022.

Williams, J. W., Van Holde, K. E., Baldwin, R. L., & Fujita, H. (1958) *Chem. Rev. 58*, 715–806.

Wu, J. R., & Lentz, B. R. (1991) *Biophys. J. 60*, 70–80.

Yphantis, D. A., Correia, J. J., Johsnon, M. L., & Wu, G. M. (1978) in *Physical Aspects of Protein Interactions* (Castimpoolas, N., Ed.) pp 275–303, Elsevier/North-Holland, New York.